



## Technical note

## Comparison of NODDI and spherical mean signal for measuring intra-neurite volume fraction

Hua Li<sup>a,\*</sup>, Rahul Nikam<sup>b</sup>, Vinay Kandula<sup>b</sup>, Ho Ming Chow<sup>a</sup>, Arabinda K. Choudhary<sup>b</sup><sup>a</sup> *Katzin Diagnostic & Research PET/MR Center, Nemours – Alfred I. duPont Hospital for Children, Wilmington, DE 19803, USA*<sup>b</sup> *Department of Radiology, Nemours – Alfred I. duPont Hospital for Children, Wilmington, DE 19803, USA*

## ARTICLE INFO

## Keywords:

Neurite orientation dispersion and density imaging (NODDI)  
 Intra-neurite volume fraction  
 Spherical mean signal

## ABSTRACT

**Purpose:** Neurite orientation dispersion and density imaging (NODDI) is a clinically feasible approach to measure intra-neurite volume fraction ( $f_{in}$ ). However, the sophisticated fitting procedure takes several hours. And the NODDI model relied on several questionable assumptions. Recent analytical work demonstrated that  $f_{in}$  could be simply calculated from the spherical mean signal (MEANS) averaged over all gradient directions with a more solid theoretical foundation. The current study aims to compare NODDI and MEANS for measuring  $f_{in}$  in human brain and investigate the potential of MEANS as a fast approach in clinics.

**Methods:** NODDI  $f_{in}$  and MEANS  $f_{in}$  were measured and compared on the same dataset. NODDI  $f_{in}$  was obtained using the NODDI MATLAB Toolbox. MEANS  $f_{in}$  is the product of the spherical mean signal and  $2\sqrt{bD}/\pi$ , where  $D$  is the intra-neurite intrinsic diffusivity.

**Results:** NODDI  $f_{in}$  and MEANS  $f_{in}$  maps are similar. The voxel-by-voxel correlation suggests that NODDI  $f_{in}$  and MEANS  $f_{in}$  are approximately equivalent to each other.

**Conclusion:** MEANS may have potential to serve a fast and simple approach to estimate  $f_{in}$  in clinics.

## 1. Introduction

Diffusion MRI has been widely used to measure tissue microstructure non-invasively. The conventional diffusion tensor imaging (DTI) technique models restricted water diffusion as a simple ellipsoid with three eigenvectors and corresponding eigenvalues [1]. The principal eigenvector is assumed to be the fiber orientation and the calculated fractional anisotropy (FA) is assumed to be an indicator of fiber density. However, it is well known that DTI is not an appropriate model in situations with crossing fibers, which commonly exist in brain white matter [2–4]. Based on the concept of high angular resolution diffusion imaging (HARDI), a large number of methods have been developed to estimate fiber orientation distribution [5–8] and fiber density [9–13]. Among them, neurite orientation dispersion and density imaging (NODDI) has been widely used to detect axonal injury in various neurological diseases [14–19] and assess neurite density changes in brain development [20–22].

NODDI is based on a three-compartment tissue model with distinct diffusion properties for each compartment [11]. The intra-neurite compartment is highly restricted for water diffusion perpendicular to neurites, and thus the intra-neurite perpendicular diffusivity is reasonably assumed to be 0. The extra-neurite compartment is also

anisotropic but less restricted than the intra-neurite compartment. The third compartment is isotropic to mimic the diffusion behavior of free water. The diffusion weighted signals are measured along different gradient directions at multiple  $b$ -values and then fit to the analytical model. From the fitting, several parameters can be derived including the intra-neurite volume fraction. Note that the number of fitted parameters depends on the complexity of the model [23].

Instead of fitting the measured signals individually, recent works have proposed to focus on the spherical mean signal averaged over all gradient directions at the same  $b$ -value [24,25]. The reason is that the spherical mean signal is independent of the fiber orientation distribution [8]. In other words, the spherical mean signal based analysis can factor out the confounding fiber orientation distribution information and reduce the number of unknown parameters in the fitting, which in turn makes the fitting procedure more robust. Because of its substantial advantage in estimating tissue microstructure, the spherical mean signal based analysis has been applied in several recent mathematical modeling studies [26–32]. The spherical mean signal based NODDI fitting was implemented efficiently and resulted in similar results with the standard NODDI fitting [27,31]. Moreover, if the diffusion weighting  $b$ -value is sufficiently large, the intra-neurite volume fraction is simply the product of the spherical mean signal and  $2\sqrt{bD}/\pi$ , where  $D$

\* Corresponding author at: Nemours AI duPont Hospital for Children, 1600 Rockland Road, 1A324, Wilmington, DE 19803, USA.

E-mail address: [hua.li@nemours.org](mailto:hua.li@nemours.org) (H. Li).

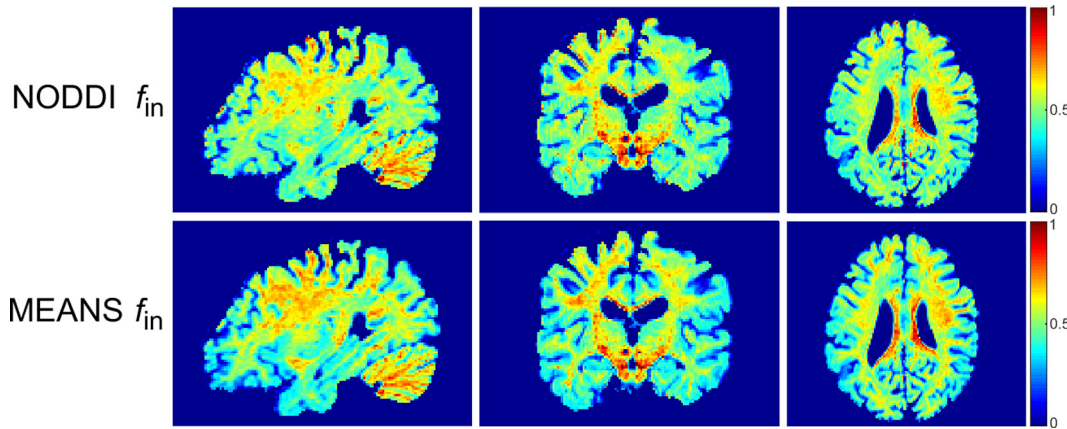


Fig. 1. The top row shows the fitted NODDI  $f_{in}$  maps from a representative HCP subject at sagittal, coronal and axial planes. The bottom row shows the corresponding MEANS  $f_{in}$  maps.

is the intra-neurite intrinsic diffusivity [33].

If the intrinsic diffusivity  $D$  is constant, as assumed in the NODDI model, the intra-neurite volume fraction can be calculated directly from the spherical mean signal without any fitting procedures. Besides, NODDI is based on several other assumptions. The fiber orientation distribution is assumed to be a single Watson distribution which could not account for fiber crossings. The extra-neurite perpendicular diffusivity is simplified with a simple tortuosity model and the extra-neurite water is modeled in fast exchange over all fiber orientations. The spherical mean signal is not affected by these assumptions. The current study aims to compare NODDI and spherical mean signal for measuring intra-neurite volume fraction and investigate the potential of spherical mean signal as a fast approach in clinics.

## 2. Materials and methods

### 2.1. Human Connectome Project (HCP) data

High-quality HCP data from 6 healthy adults, as part of the MGH-USC Adult Diffusion Dataset, were downloaded from ConnectomeDB (<http://db.humanconnectome.org>). Diffusion data were acquired with 4 different  $b$ -values ranging from  $1 \text{ ms}/\mu\text{m}^2$  to  $10 \text{ ms}/\mu\text{m}^2$ , but only  $b = 1 \text{ ms}/\mu\text{m}^2$  and  $b = 3 \text{ ms}/\mu\text{m}^2$  were used in the current study. The number of gradient directions was 64 at each shell and the number of  $b = 0$  images was 10. Other imaging parameters were: repetition time (TR) = 8800 ms, echo time (TE) = 57 ms, gradient duration ( $\delta$ ) = 12.9 ms, gradient separation ( $\Delta$ ) = 21.8 ms, image resolution =  $1.5 \times 1.5 \times 1.5 \text{ mm}^3$ , parallel imaging acceleration factor = 3, and multiband factor = 1. The data were preprocessed with corrections for gradient nonlinearity distortions, head motion, and eddy current artifacts [34]. All the 10  $b = 0$  images were averaged and then segmented to gray matter (GM), white matter (WM) and cerebrospinal fluid (CSF) using FSL *fast* command [35,36].

### 2.2. Data analysis

As modeled in NODDI, the diffusion weighted signal ( $S$ ) measured along gradient direction  $\mathbf{g}$  can be written as

$$S(\mathbf{b}, \mathbf{g}) = S_0 \cdot [f_{in} \cdot S_{in}(\mathbf{b}, \mathbf{g}) + (1 - f_{in} - f_{iso}) \cdot S_{ex}(\mathbf{b}, \mathbf{g}) + f_{iso} \cdot S_{iso}(\mathbf{b})] \quad (1)$$

where  $S_0$  is the signal for  $b = 0$ ;  $S_{in}$  and  $f_{in}$  are the normalized signal and volume fraction of the intra-neurite compartment;  $S_{ex}$  is the normalized signal of the extra-neurite compartment; and  $S_{iso}$  and  $f_{iso}$  are the normalized signal and volume fraction of the CSF compartment. The intra-neurite intrinsic diffusivity  $D$  is fixed as  $1.7 \mu\text{m}^2/\text{ms}$ . Details of other assumptions can be found in the original work [11], which have also been discussed in several recent studies [26,27,37,38]. NODDI  $f_{in}$  was

obtained using the NODDI MATLAB Toolbox.

When the diffusion weighting  $b$ -value is sufficiently large ( $b \geq 3 \text{ ms}/\mu\text{m}^2$ ) [33], the extra-neurite water contribution is negligible and the spherical mean diffusion weighted signal ( $\bar{S}$ ) can be expressed as.

$$\bar{S}(b) = S_0 f_{in} \cdot \frac{\sqrt{\pi}}{2\sqrt{bD}} \quad (2)$$

Here the  $\bar{S}$ -based  $f_{in}$  is termed MEANS  $f_{in}$ . Only  $b = 3 \text{ ms}/\mu\text{m}^2$  was used in Eq. (2) to calculate MEANS  $f_{in}$ . The Rician bias was reduced by using the adjusted signal  $\sqrt{S^2(\mathbf{b}, \mathbf{g}) - \sigma^2}$  [25,39], where  $\sigma$  is the median of the standard deviation calculated voxel-by-voxel from all the  $b = 0$  images.

### 2.3. Clinical data

As a supplementary analysis, NODDI  $f_{in}$  and MEANS  $f_{in}$  were further compared on clinical data. Three children (12–36 months, 2 boys) with focal cortical dysplasia at Nemours/Alfred I. duPont Hospital for Children were retrospectively selected for the analysis. Two children were scanned on a 3 T GE MR750 scanner, and the other one was scanned on a GE SIGNA PET/MR scanner using the same diffusion protocol. The  $b$ -values were 1, 2 and  $3 \text{ ms}/\mu\text{m}^2$  with 15, 20 and 25 gradient directions, respectively. The number of  $b = 0$  images was 6. Other diffusion imaging parameters were: TR = 9700 ms, TE = 99 ms, number of slices = 56, slice thickness = 2.5 mm, field of view =  $240 \times 240 \text{ mm}^2$ , in-plane image resolution =  $2.5 \times 2.5 \text{ mm}^2$ , and parallel imaging acceleration factor = 2. Diffusion images were preprocessed with corrections for head motion, and eddy current artifacts using FSL *eddy* command [40]. NODDI  $f_{in}$  and MEANS  $f_{in}$  were obtained subsequently following the above data analysis. T1 weighted, T2 weighted and T2 FLAIR structural images were co-registered to the mean  $b = 0$  image using FSL *flirt* command [41]. The study was approved by local Institutional Review Board.

## 3. Results

Fig. 1 shows the NODDI  $f_{in}$  and MEANS  $f_{in}$  maps acquired from a representative HCP subject at three anatomical planes. The two methods result in similar contrast. Consistent with previous NODDI studies [11,27,31], the value of  $f_{in}$  is higher in white matter than in gray matter.

Fig. 2 shows the correlation between NODDI  $f_{in}$  and MEANS  $f_{in}$ . The density plot is from all gray matter and white matter voxels of the same subject shown in Fig. 1. Red denotes higher density of points, and blue denotes lower density. The solid line indicates the result of linear least squares fitting. The fitting slope is close to 1 and the intercept is close to

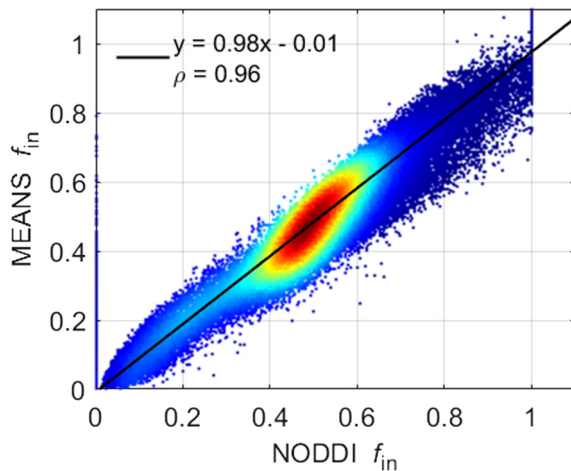


**Fig. 2.** Density scatter plot and Pearson correlation between NODDI  $f_{in}$  and MEANS  $f_{in}$  using all gray matter and white matter voxels of the same subject shown in Fig. 1. Red denotes higher density of points, and blue denotes lower density. The solid line indicates the result of linear least squares fitting. (For interpretation of the references to colour in this figure legend, the reader is referred to the web version of this article.)

0. Pearson's linear correlation coefficient ( $\rho$ ) is also provided. The correlation coefficient  $\rho = 0.96 \pm 0.01$  over six HCP subjects. Fig. 2 suggests that NODDI  $f_{in}$  and MEANS  $f_{in}$  are approximately equivalent to each other.

Fig. 3 shows representative structural images, NODDI  $f_{in}$ , MEANS  $f_{in}$ , and the absolute difference between NODDI  $f_{in}$  and MEANS  $f_{in}$  ( $|f_{in}(\text{NODDI}) - f_{in}(\text{MEANS})|$ ) acquired from a patient with focal cortical dysplasia. Structural images demonstrate subtle cortical dysplasia in the right cerebral hemisphere as evidenced by poor gray-white matter differentiation and T2 hyper-intense signal. The cortical dysplasia lesion region is outlined with red curve in Fig. 3 (b). Consistent with previous NODDI work [18], the lesion shows reduced NODDI  $f_{in}$  compared with the contralateral side. Fig. 3 (e) suggests that MEANS  $f_{in}$  has slightly better contrast than NODDI  $f_{in}$  in this patient. The whole brain mean  $|f_{in}(\text{NODDI}) - f_{in}(\text{MEANS})|$  is  $0.026 \pm 0.002$  over three patients and the difference is more significant in gray matter than in

white matter.

#### 4. Discussion

The current study compared NODDI and MEANS for measuring intra-neurite volume fraction on the same human brain data. Both methods are based on multi-compartment tissue modeling. NODDI fits the measured diffusion weighted signals to the analytical model individually. Instead, MEANS focuses on the spherical mean signal and derives intra-neurite volume fraction from spherical mean signal directly. The comparison results suggest that NODDI  $f_{in}$  and MEANS  $f_{in}$  are approximately equivalent. It should be noted that the current study is not aimed to assess which method is more accurate. Without the information of ground truth, it is unable to assess their accuracy. However, the comparison of different methods may help investigate their similarities and differences.

Compared with NODDI, MEANS is based on a more solid theoretical foundation. NODDI assumes a simple fiber orientation distribution and models the extra-neurite water diffusion in specific form. MEANS is not affected by these assumptions. NODDI and MEANS share two common assumptions: 1) the intra-neurite perpendicular diffusivity is 0 and 2) the intra-neurite intrinsic diffusivity  $D$  is constant over the whole brain. Due to the small restricting size [42] and long diffusion time on human scanner [9,43], the first assumption is usually agreed to be reasonable. Recent power law scaling studies demonstrated that the spherical mean signal decay behavior is consistent with Eq. (2) in white matter [37,44]. However, the spherical mean signal decay in gray matter is substantially faster, which makes the first assumption inappropriate for microstructural modeling in gray matter [37,44]. Water permeability [37] and fiber curvedness [45] have been proposed to explain the gray/white matter difference. Thus, the accuracy of  $f_{in}$  quantification in gray matter is compromised by the first assumption. Though the measured NODDI  $f_{in}$  or MEANS  $f_{in}$  is not accurate in gray matter, it may still be able to provide some useful information about structural changes [46,47]. As for the second assumption, it is evident from Eq. (2) that the calculated MEANS  $f_{in}$  will be biased when the assumption is violated. A recent study [48] found that the intra-neurite intrinsic diffusivity  $D$  is about  $2.25 \mu\text{m}^2/\text{ms}$  rather than  $1.7 \mu\text{m}^2/\text{ms}$  as assumed by NODDI. MEANS  $f_{in}$  would increase by 15% when the intrinsic diffusivity  $D$  changes from  $1.7 \mu\text{m}^2/\text{ms}$  to  $2.25 \mu\text{m}^2/\text{ms}$ . And NODDI  $f_{in}$  is expected to

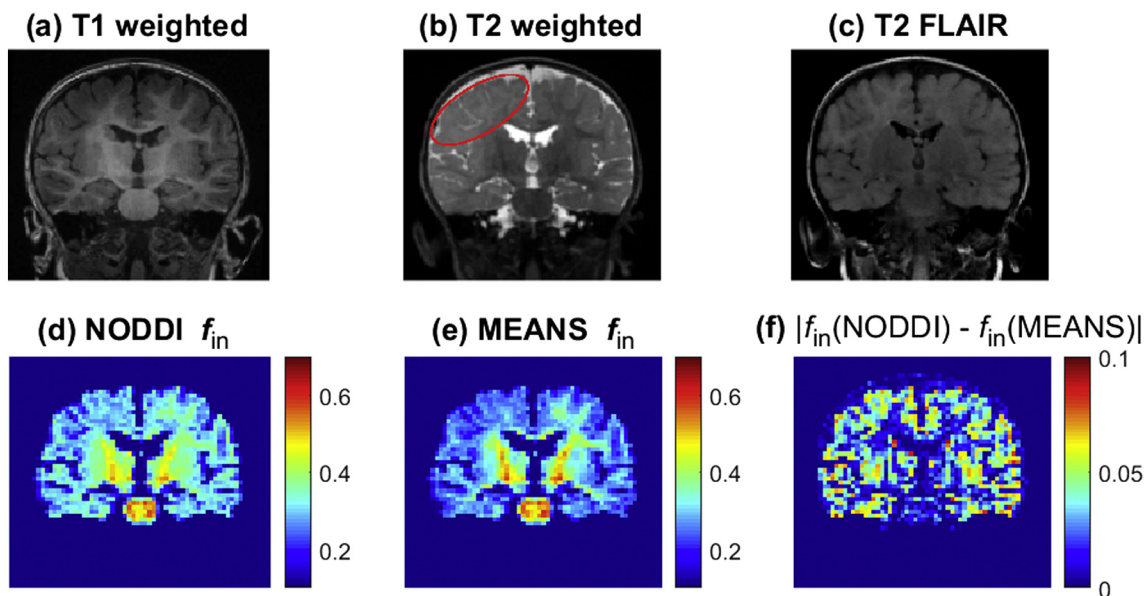


**Fig. 3.** Images of T1 weighted (a), T2 weighted (b), T2 FLAIR (c), NODDI  $f_{in}$  (d), MEANS  $f_{in}$  (e) and the absolute difference between NODDI  $f_{in}$  and MEANS  $f_{in}$  (f) acquired from a representative patient with focal cortical dysplasia. The red curve in (b) outlines the cortical dysplasia lesion. (For interpretation of the references to colour in this figure legend, the reader is referred to the web version of this article.)

be affected similarly. Several studies have proposed to estimate  $f_{in}$  and  $D$  simultaneously using multi-shell diffusion data [26,28–30,32] or novel diffusion sequences [27,49], but the results have not been validated yet. An accurate measurement of  $D$  would assist in better understanding the strengths and limitations of NODDI and MEANS.

The main difference between NODDI and MEANS is that NODDI requires at least two  $b$  shells. Besides  $f_{in}$ , NODDI provides two more valuable indices: fiber orientation dispersion index ODI and isotropic water volume fraction  $f_{iso}$  [11]. As mentioned in the original NODDI work [11], ODI can be estimated with just a single shell. Hence, the single shell data used in MEANS can also be used to estimate ODI through the standard NODDI fitting. Alternatively, the single shell data can be used to obtain the full fiber orientation distribution [50], which in turn can be used to calculate the orientation dispersion entropy [26]. The simultaneous fitting of  $f_{in}$  and  $f_{iso}$  indeed requires at least two shells. But previous studies observed an overestimated NODDI  $f_{iso}$  in white matter [11,27]. A simple biexponential-T2 approach may estimate  $f_{iso}$  more accurately [51].

NODDI protocol has been optimized and investigated through simulations extensively [11,21,22,52]. It was shown that the maximal  $b$ -value could be reduced to  $2 \text{ ms}/\mu\text{m}^2$  without significant effect on the estimated parameters [11]. As for MEANS, a high  $b$ -value ( $\sim 3 \text{ ms}/\mu\text{m}^2$ ) [9] or even higher [37,44] is required to fully suppress the extra-neurite water contribution. The effect of  $b$ -value and number of gradient directions on the accuracy of MEANS  $f_{in}$  has been investigated recently [30,37,53,54]. The measured signal at  $b = 3 \text{ ms}/\mu\text{m}^2$  is highly correlated with that at  $b = 5 \text{ ms}/\mu\text{m}^2$  for human brain white matter, which suggests that  $b = 3 \text{ ms}/\mu\text{m}^2$  is sufficient for spherical mean signal based studies in human brain white matter [53]. And it was recommended to use  $10 \times b/b_1$  ( $b_1 = 1 \text{ ms}/\mu\text{m}^2$ ) uniformly distributed gradient directions for typical human diffusion studies with signal-to-noise ratio  $\sim 20$  [54].

Compared with NODDI, MEANS  $f_{in}$  shows greater potential for clinical applications. First,  $\bar{S}$ -based data analysis is independent of fiber orientation distribution [8,25], MEANS  $f_{in}$  is likely to be more accurate than NODDI  $f_{in}$ . Second, MEANS estimates only one parameter. Diffusion-based microstructural modeling is generally associated with low signal-to-noise ratio and low image resolution [46,55]. Multi-shell diffusion data are needed to estimate extra parameters [11,26,29]. High resolution MEANS  $f_{in}$  map is achievable by increasing the number of gradient directions at a single  $b$ -value. And the consequential signal-to-noise ratio is expected to be proportional to the square root of the number of gradient directions [49,54]. Third, the contrast is the same with the arithmetic mean signal, which may be generated on the scanner and read by radiologists soon after the scan is complete.

## 5. Conclusion

NODDI and MEANS were compared for measuring intra-neurite volume fraction in human brain. The voxel-by-voxel correlation suggests that NODDI  $f_{in}$  and MEANS  $f_{in}$  are approximately equivalent to each other. Without the need of sophisticated fitting, MEANS may have potential to serve a fast and simple approach to estimate  $f_{in}$  in clinics.

## Acknowledgements

This work was supported by the National Institutes of Health (grant number R21DC015853). Data were provided by the Human Connectome Project, MGH-USC Consortium (Principal Investigators: Bruce R. Rosen, Arthur W. Toga and Van Wedeen; U01MH093765) funded by the NIH Blueprint Initiative for Neuroscience Research grant; the National Institute of Health, United States grant P41EB015896; and the Instrumentation Grants S10RR023043, 1S10RR023401, 1S10RR019307.

## References

- [1] Basser PJ, Mattiello J, LeBihan D. MR diffusion tensor spectroscopy and imaging. *Biophys J* 1994;66:259–67. [https://doi.org/10.1016/S0006-3495\(94\)80775-1](https://doi.org/10.1016/S0006-3495(94)80775-1).
- [2] Leow AD, Zhan L, Zhu S, Hageman N, Chiang MC, Barysheva M, et al. White matter integrity measured by fractional anisotropy correlates poorly with actual individual fiber anisotropy. *Proc. - 2009 IEEE Int. Symp. Biomed. Imaging From Nano to Macro, ISBI 2009* 2009. p. 622–5. <https://doi.org/10.1109/ISBI.2009.5193124>.
- [3] Schilling K, Gao Y, Janve V, Stepniewska I, Landman BA, Anderson AW. Can increased spatial resolution solve the crossing fiber problem for diffusion MRI? *NMR Biomed* 2017;30. <https://doi.org/10.1002/nbm.3787>.
- [4] Jones DK, Knösche TR, Turner R. White matter integrity, fiber count, and other fallacies: the  $\text{ndo}$ 's and  $\text{don'ts}$  of diffusion MRI. *NeuroImage* 2013;73:239–54. <https://doi.org/10.1016/j.neuroimage.2012.06.081>.
- [5] Tuch DS, Reese TG, Wiegell MR, Makris N, Belliveau JW, Van Wooten J. High angular resolution diffusion imaging reveals intravoxel white matter fiber heterogeneity. *Magn Reson Med* 2002;48:577–82. <https://doi.org/10.1002/mrm.10268>.
- [6] Behrens TEJ, Woolrich MW, Jenkinson M, Johansen-Berg H, Nunes RG, Clare S, et al. Characterization and propagation of uncertainty in diffusion-weighted MR imaging. *Magn Reson Med* 2003;50:1077–88. <https://doi.org/10.1002/mrm.10609>.
- [7] Tournier JD, Calamante F, Gadian DG, Connelly A. Direct estimation of the fiber orientation density function from diffusion-weighted MRI data using spherical deconvolution. *NeuroImage* 2004;23:1176–85. <https://doi.org/10.1016/j.neuroimage.2004.07.037>.
- [8] Anderson AW. Measurement of fiber orientation distributions using high angular resolution diffusion imaging. *Magn Reson Med* 2005;54:1194–206. <https://doi.org/10.1002/mrm.20667>.
- [9] Raffelt D, Tournier JD, Rose S, Ridgway GR, Henderson R, Crozier S, et al. Apparent fibre density: a novel measure for the analysis of diffusion-weighted magnetic resonance images. *NeuroImage* 2012;59:3976–94. <https://doi.org/10.1016/j.neuroimage.2011.10.045>.
- [10] Fieremans E, Jensen JH, Helpert JA. White matter characterization with diffusional kurtosis imaging. *NeuroImage* 2011;58:177–88. <https://doi.org/10.1016/j.neuroimage.2011.06.006>.
- [11] Zhang H, Schneider T, Wheeler-Kingshott CA, Alexander DC. NODDI: practical in vivo neurite orientation dispersion and density imaging of the human brain. *NeuroImage* 2012;61:1000–16. <https://doi.org/10.1016/j.neuroimage.2012.03.072>.
- [12] Jespersen SN, Kroenke CD, Ostergaard L, Ackerman JJH, Yablonskiy DA. Modeling dendrite density from magnetic resonance diffusion measurements. *NeuroImage* 2007;34:1473–86. <https://doi.org/10.1016/j.neuroimage.2006.10.037>.
- [13] Jespersen SN, Bjarkam CR, Nyengaard JR, Chakravarty MM, Hansen B, Vosegaard T, et al. Neurite density from magnetic resonance diffusion measurements at ultrahigh field: comparison with light microscopy and electron microscopy. *NeuroImage* 2010;49:205–16. <https://doi.org/10.1016/j.neuroimage.2009.08.053>.
- [14] Adluru G, Gur Y, Anderson JS, Richards LG, Adluru N, Dibella EVR. Assessment of white matter microstructure in stroke patients using NODDI. *Conf Proc IEEE Eng Med Biol Soc* 2014. IEEE Eng Med Biol Soc Annu Conf; 2014. p. 742–5. <https://doi.org/10.1109/EMBC.2014.6943697>.
- [15] Churchill NW, Caverzasi E, Graham SJ, Hutchison MG, Schweizer TA. White matter microstructure in athletes with a history of concussion: comparing diffusion tensor imaging (DTI) and neurite orientation dispersion and density imaging (NODDI). *Hum Brain Mapp* 2017;38:4201–11. <https://doi.org/10.1002/hbm.23658>.
- [16] Schneider T, Brownlee W, Zhang H, Ciccarelli O, Miller DH, Wheeler-Kingshott CG. Sensitivity of multi-shell NODDI to multiple sclerosis white matter changes: a pilot study. *Funct Neurol* 2017;32:97–101. <https://doi.org/10.11138/FNeur/2017.32.2.097>.
- [17] Slattery CF, Zhang J, Paterson RW, Foulkes AJM, Carton A, Macpherson K, et al. ApoE influences regional white-matter axonal density loss in Alzheimer's disease. *Neurobiol Aging* 2017;57:8–17. <https://doi.org/10.1016/j.neurobiolaging.2017.04.021>.
- [18] Winston GP, Micallef C, Symms MR, Alexander DC, Duncan JS, Zhang H. Advanced diffusion imaging sequences could aid assessing patients with focal cortical dysplasia and epilepsy. *Epilepsy Res* 2014;108:336–9. <https://doi.org/10.1016/j.epilepsyres.2013.11.004>.
- [19] By S, Xu J, Box BA, Bagnato FR, Smith SA. Application and evaluation of NODDI in the cervical spinal cord of multiple sclerosis patients. *NeuroImage Clin* 2017;15:333–42. <https://doi.org/10.1016/j.nicl.2017.05.010>.
- [20] Kunz N, Zhang H, Vasung L, O'Brien KR, Assaf Y, Lazeyras F, et al. Assessing white matter microstructure of the newborn with multi-shell diffusion MRI and biophysical compartment models. *NeuroImage* 2014;96:288–99. <https://doi.org/10.1016/j.neuroimage.2014.03.057>.
- [21] Kodiweera C, Alexander AL, Harezlak J, McAllister TW, Wu YC. Age effects and sex differences in human brain white matter of young to middle-aged adults: a DTI, NODDI, and q-space study. *NeuroImage* 2016;128:180–92. <https://doi.org/10.1016/j.neuroimage.2015.12.033>.
- [22] Jelescu IO, Veraart J, Adisetiyo V, Milla SS, Novikov DS, Fieremans E. One diffusion acquisition and different white matter models: how does microstructure change in human early development based on WMTI and NODDI? *NeuroImage* 2015;107:242–56. <https://doi.org/10.1016/j.neuroimage.2014.12.009>.
- [23] Tariq M, Schneider T, Alexander DC, Gandini Wheeler-Kingshott CA, Zhang H. Bingham-NODDI: mapping anisotropic orientation dispersion of neurites using diffusion MRI. *NeuroImage* 2016;133:207–23. <https://doi.org/10.1016/j.neuroimage.2016.01.046>.

- [24] Jespersen SN, Lundell H, S nderby CK, Dyrby TB. Orientationally invariant metrics of apparent compartment eccentricity from double pulsed field gradient diffusion experiments. *NMR Biomed* 2013;26:1647–62. <https://doi.org/10.1002/nbm.2999>.
- [25] Kaden E, Kruggel F, Alexander DC. Quantitative mapping of the per-axon diffusion coefficients in brain white matter. *Magn Reson Med* 2016;75:1752–63. <https://doi.org/10.1002/mrm.25734>.
- [26] Kaden E, Kelm ND, Carson RP, Does MD, Alexander DC. Multi-compartment microscopic diffusion imaging. *NeuroImage* 2016;139:346–59. <https://doi.org/10.1016/j.neuroimage.2016.06.002>.
- [27] Lampinen B, Szczepankiewicz F, M rtensson J, van Westen D, Sundgren PC, Nilsson M. Neurite density imaging versus imaging of microscopic anisotropy in diffusion MRI: a model comparison using spherical tensor encoding. *NeuroImage* 2017;147:517–31. <https://doi.org/10.1016/j.neuroimage.2016.11.053>.
- [28] Reisert M, Kellner E, Dhital B, Hennig J, Kiselev VG. Disentangling micro from mesostructure by diffusion MRI: a Bayesian approach. *NeuroImage* 2017;147:964–75. <https://doi.org/10.1016/j.neuroimage.2016.09.058>.
- [29] Novikov DS, Veraart J, Jelescu IO, Fieremans E. Rotationally-invariant mapping of scalar and orientational metrics of neuronal microstructure with diffusion MRI. *NeuroImage* 2018. <https://doi.org/10.1016/j.neuroimage.2018.03.006>.
- [30] McKinnon ET, Helpert JA, Jensen JH. Modeling white matter microstructure with fiber ball imaging. *NeuroImage* 2018. <https://doi.org/10.1016/j.neuroimage.2018.04.025>.
- [31] Zucchelli M, Descoteaux M, Menegaz G. NODDI-SH: a computational efficient NODDI extension for fODF estimation in diffusion MRI. *arXiv Prepr. arXiv1708.08999*. 2017.
- [32] Veraart J, Novikov DS, Fieremans E. TE dependent diffusion imaging (TEdDI) distinguishes between compartmental T2relaxation times. *NeuroImage* 2017. <https://doi.org/10.1016/j.neuroimage.2017.09.030>.
- [33] Jensen JH, Russell Glenn G, Helpert JA. Fiber ball imaging. *NeuroImage* 2016;124:824–33. <https://doi.org/10.1016/j.neuroimage.2015.09.049>.
- [34] Fan Q, Witzel T, Nummenmaa A, Van Dijk KRA, Van Horn JD, Drews MK, et al. MGH-USC human connectome project datasets with ultra-high b-value diffusion MRI. *NeuroImage* 2016;124:1108–14. <https://doi.org/10.1016/j.neuroimage.2015.08.075>.
- [35] Zhang Y, Brady M, Smith S. Segmentation of brain MR images through a hidden Markov random field model and the expectation-maximization algorithm. *IEEE Trans Med Imaging* 2001;20:45–57. <https://doi.org/10.1109/42.906424>.
- [36] Smith SM, Jenkinson M, Woolrich MW, Beckmann CF, Behrens TEJ, Johansen-Berg H, et al. Advances in functional and structural MR image analysis and implementation as FSL. *NeuroImage* 2004;vol. 23. <https://doi.org/10.1016/j.neuroimage.2004.07.051>.
- [37] McKinnon ET, Jensen JH, Glenn GR, Helpert JA. Dependence on b-value of the direction-averaged diffusion-weighted imaging signal in brain. *Magn Reson Imaging* 2017;36:121–7. <https://doi.org/10.1016/j.mri.2016.10.026>.
- [38] Novikov DS, Kiselev VG, Jespersen SN. On modeling. *Magn Reson Med* 2018;79:3172–93. <https://doi.org/10.1002/mrm.27101>.
- [39] Gudbjartsson H, Patz S. The rician distribution of noisy mri data. *Magn Reson Med* 1995;34:910–4. <https://doi.org/10.1002/mrm.1910340618>.
- [40] Andersson JLR, Sotiropoulos SN. An integrated approach to correction for off-resonance effects and subject movement in diffusion MR imaging. *NeuroImage* 2016;125:1063–78. <https://doi.org/10.1016/j.neuroimage.2015.10.019>.
- [41] Jenkinson M, Bannister P, Brady M, Smith S. Improved optimisation for the robust and accurate linear registration and motion correction of brain images. *NeuroImage* 2002;17:825–41. [https://doi.org/10.1016/S1053-8119\(02\)91132-8](https://doi.org/10.1016/S1053-8119(02)91132-8).
- [42] Lieuwald D, Miller R, Logothetis N, Wagner HJ, Sch uz A. Distribution of axon diameters in cortical white matter: an electron-microscopic study on three human brains and a macaque. *Biol Cybern* 2014;108:541–57. <https://doi.org/10.1007/s00422-014-0626-2>.
- [43] Jiang X, Li H, Xie J, Zhao P, Gore JC, Xu J. Quantification of cell size using temporal diffusion spectroscopy. *Magn Reson Med* 2016;75:1076–85. <https://doi.org/10.1002/mrm.25684>.
- [44] Veraart J, Fieremans E, Novikov DS. Universal power-law scaling of water diffusion in human brain defines what we see with MRI. *arXiv Prepr. arXiv1609.09145*. 2016.
- [45]  zarslan E, Yolcu C, Herberthson M, Knutsson H, Westin C-F. Influence of the size and curvedness of neural projections on the orientationally averaged diffusion MR signal. *Front Phys* 2018;6. <https://doi.org/10.3389/fphy.2018.00017>.
- [46] Rostampour M, Hashemi H, Najibi SM, Oghabian MA. Detection of structural abnormalities of cortical and subcortical gray matter in patients with MRI-negative refractory epilepsy using neurite orientation dispersion and density imaging. *Phys Med* 2018;48:47–54. <https://doi.org/10.1016/j.ejmp.2018.03.005>.
- [47] Gen c E, Fraenz C, Schl ter C, Friedrich P, Hossiep R, Voelkle MC, et al. Diffusion markers of dendritic density and arborization in gray matter predict differences in intelligence. *Nat Commun* 2018;9. <https://doi.org/10.1038/s41467-018-04268-8>.
- [48] Dhital B, Reisert M, Kellner E, Kiselev VG. Intra-axonal diffusivity in brain white matter. *arXiv Prepr. arXiv1712.04565*. 2017.
- [49] Jensen JH, Helpert JA. Characterizing intra-axonal water diffusion with direction-averaged triple diffusion encoding MRI. *NMR Biomed* 2018;31. <https://doi.org/10.1002/nbm.3930>.
- [50] Tournier JD, Calamante F, Connelly A. Robust determination of the fibre orientation distribution in diffusion MRI: non-negativity constrained super-resolved spherical deconvolution. *NeuroImage* 2007;35:1459–72. <https://doi.org/10.1016/j.neuroimage.2007.02.016>.
- [51] Ferizi U, Scherrer B, Schneider T, Alipoor M, Eufrazio O, Fick RHJ, et al. Diffusion MRI microstructure models with in vivo human brain connectome data: results from a multi-group comparison. *NMR Biomed* 2017;30. <https://doi.org/10.1002/nbm.3734>.
- [52] Kamiya K, Hori M, Irie R, Miyajima M, Nakajima M, Kamagata K, et al. Diffusion imaging of reversible and irreversible microstructural changes within the corticospinal tract in idiopathic normal pressure hydrocephalus. *NeuroImage Clin* 2017;14:663–71. <https://doi.org/10.1016/j.nicl.2017.03.003>.
- [53] Li H, Chow HM, Chugani DC, Chugani HT. Linking spherical mean diffusion weighted signal with intra-axonal volume fraction. *Magn Reson Imaging* 2018. <https://doi.org/10.1016/j.mri.2018.11.006>.
- [54] Li H, Chow HM, Chugani DC, Chugani HT. Minimal number of gradient directions for robust measurement of spherical mean diffusion weighted signal. *Magn Reson Imaging* 2018;54:148–52. <https://doi.org/10.1016/j.mri.2018.08.020>.
- [55] Chougar L, Hagiwara A, Maekawa T, Hori M, Andica C, Iimura Y, et al. Limitation of neurite orientation dispersion and density imaging for the detection of focal cortical dysplasia with a “transmantle sign”. *Phys Med* 2018;52:183–4.